6th International Symposium on Three-Dimensional Electromagnetics
Berkeley, California, USA, March 28-30, 2017

Plausibility of monitoring hydrofracturing with electromagnetic array: Suggestions from 3D numerical simulation

Lanbo Liu[1] and Mark D. Zoback[2]
[1]Department of Civil & Environmental Engineering, University of Connecticut
[2]Department of Geophysics, Stanford University

SUMMARY

Up to date the microseismic method is the major tool for hydrofracturing monitoring in petroleum industry. In this paper we examine the plausibility of characterizing the effectiveness of the hydrofracturing process by looking into the extent of the electric conductivity variations by continuous magnetotelluric surveys during the hydrofracturing stage increment through numerical simulation. The numerical simulation results suggest that it is possible to characterize the extent of the volume of hydrofractured stages based the changes in apparent resistivity expressed by the impedance tensor.

Keywords: numerical simulation, magnetotelluric surveys, hydrofracturing, impedance tensor, apparent resistivity

INTRODUCTION

Recent petroleum exploration and development activities in the US and around the world have put a significant portion of effort on unconventional resources, which predominantly consist of low-permeability siltstones and shale reservoirs. Multi-stage hydrofracturing aimed to achieve sufficient flow in reservoir formations is one of a few key technologies to economically produce oil and gas. One major parameter for hydrofracturing effectiveness characterization is the extent of the induced fracture zones. This parameter is critical to unconventional resources development process, but is depicted with high uncertainties by the monitoring techniques available up to date. Currently, the majority of the effort involves recording passive seismic events to locating the micro-seismicity, along with detecting ground surface deformation. Passive seismic uses surface or borehole geophones to detect microseicmic events generated during the fracturing process. Data are then used to infer the location and orientation of the induced fractures. The method has been effective in fields where brittle reservoirs mark the fracture path with seismic events (Maxwell et al., 2012, Albaric et al., 2013). In less brittle reservoirs, or in fields where natural fractures play a role, the recorded events are less diagnostic. Moreover, microseicmic activities is not directly sensitive to the fluids present within those Fractures. Thus, it is difficult to gain any information regarding the permeability or fluid motion occurring at depth. With ground deformation, the displacement is measured at the surface or in shallow boreholes using precision tiltmeters. Data are interpreted to map the fracture orientation and displacement from the 'bulge' induced by volume change by fluid injection. The method has been effective in shallow reservoirs, but it suffers from poor sensitivity to deeper fractures and in the non-uniqueness of reconstructions (Warpinski, 2011, Pandurangan et al 2015).

Using electromagnetic (EM) array measurements the natural EM field around and below 1 Hz is another viable way to expand the means for hydrofracturing characterization in deep formations. A few field detection for using EM array to monitor the hydrofracturing process have been documented recently (MacFarlane, et al, 2014; He et al 2015; Didana, et al 2016; Thiel, S., 2016). However, efficiently model the EM response to the hydrofracturing process at a realistic field scale poses great challenge for forward simulation, and consequently in solving the inverse problem.

In this paper we use three-dimensional (3D) finite difference time domain (FDTD) numerical simulation tool and the effective medium theory (EMT) to test the plausibility of using magnetotelluric EM surveys for this application by looking into the variations of the electromagnetic parameters accompanying with the growth of the hydraulically fractured zones by stage advancement. The key assumption is that the proppant is electrically distinctive from the host reservoir formation rocks with higher electric conductivity and higher dielectric permittivity (Archie, 1942; Glover, 2010). We basically followed the approach proposed by Mittet (2010) in which a correspondence principle of wave and diffusion fields is used to formulate out a mathematic approach to convert the diffusion equation for the low-frequency EM field in a conductive medium to a fictitious wave equation for the high-frequency EM wave propagation in a resistive, dielectric medium through the link of a reference frequency ω_0. By employing this transform, the low-frequency diffusive EM field can be modelled by a fictitious EM wave for modelling efficiency and then transform back to the low-frequency field for physical interpretation.

We applied this approach and selected a reference frequency value and generated the synthetic Green's function for mimic the EM wave energy in the MT frequency band for modelling the EM response to multi-stage hydrofracturing by adopting the fictitious wave field simulation. The results can be transformed back to the diffusion domain by applying the wave-diffusion correspondence principle in a later process.

MODELING STRATEGY

To model the magnetotelluric resources we use the pseudo-spectral time domain (PSTD) method (Liu and Arcone, 2005) to simulate the case of an impulse plane EM wave vertically impinging the earth with a central frequency of 1 Hz. The major parameters and approaches are laid out below. This kind of setup is inspired by some typical magnetotelluric surveys conducted to monitoring the development of fracture zones in a number of field deployments for geothermal resources and shale gas plays. Figure 1 shows a typical field deployment for MT survey (e.g., Thiel, 2016) as an example.

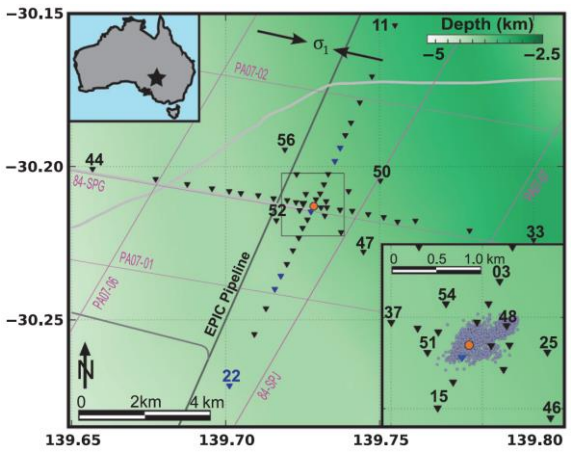

Figure 1. Survey layout of the MT sites (triangles) across the 3.7 km deep borehole (red circle) of the Paralana enhanced geothermal systems, South Australia. Inset shows microseimic events recorded during fracking. Background color is depth to basement (Thiel, 2016).

Material properies

A generic setup of multi-stage hydrofracturing process operated from a horizontal segment of a borehole in the source layer is shown in Figure 2. We constructed a numerical model domain with a volume of 2560×2560×2560 cubic meters with a cell size of 10 meters that contains the source formation and the hydrofracturing stages sandwiched between the isotropic overlying and underlying formations (Figure 3). We defined the materials above and below the target formation as a homogeneous, isotropic medium with a dielectric constant value of 6. The source formation of shales is modelled as the horizontally transverse isotropic (HTI) medium with the major axis in X-direction (Figure 3).

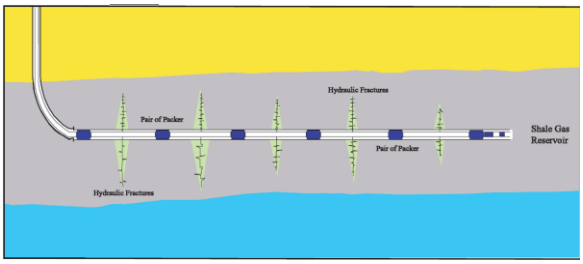

Figure 2. An illustration of the multi-stage hydraulic fracturing in the shale source layer (Abdulaziz, 2013).

Each of the hydrofracturing stage creates a fractured zone in the shape of an ellipsoid with semi-axes of 200 m (in Y-direction), 100 m (in Z-direction) and 15 m (in X-direction). The spacing interval between two adjacent stages is 100 m. Hydro-fractured zones have an effective dielectric constant of 9, increased by 28% from the background of 7 for the reservoir layer.

The array formed by the measuring points in the numerical model are placed on the earth surface and can be distributed in any arbitrary fashion to form interferometric pairs to investigate the optimistic configuration of the field observation arrays. However, in this synthetic investigation there are 24×24=576 measuring points to be used to record the horizontal components of both the electric field and the magnetic field (i.e., E_x, E_y, H_x, and H_y).

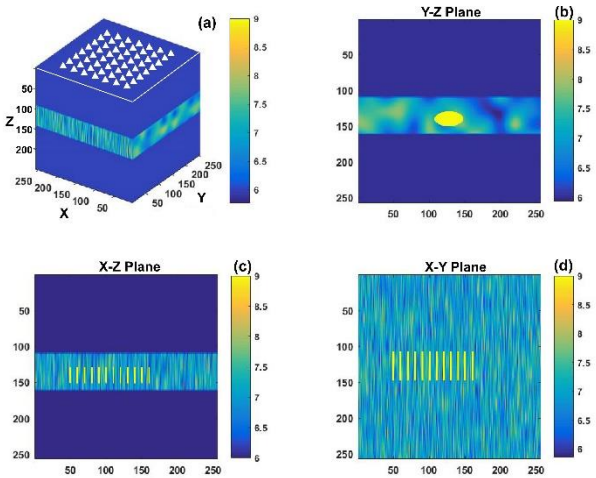

Figure 3. The formation model in terms of the dielectric constant ε_r with 12 hydrofracturing stages and the location of the receiving array on the surface. (a) the 3D view of the model; (b) the view in Y-Z plane through a fractured stage near the center of x=(nx×dx)/2; (c) the view in X-Z plane through y=(ny×dy)/2; (d) the view in X-Y plane through z=(nz×dz)/2. The group of the 12 fractured stages with ε_r=9 can be seen in (c) and (d).

Selection of frequency band

Penetration of the EM wave to the target depth can be essentially characterized by the concept of skin depth δ (in meters):

$$\delta = \sqrt{\frac{2}{\omega\sigma\mu}} \approx \frac{503}{\sqrt{f \cdot \sigma}} \qquad (1)$$

The frequency range suitable to give the best resolution with sufficient signal to noise ratio for the target depth less than 5 km is 0.1-1 Hz. For testing the modelling validity we used the impulse source with the selection of the central frequency 1 Hz, with an effective band width of 0.5–3 Hz. It is literally a plane wave with a wavelength at the order of magnitude of 10^8 meters. To model such a plane wave with Mittet's (2010) approach we have chosen a reference frequency of 9×10^{-5} Hz to get a fictitious wave travel in the fictitious media at a fictitious speed of 300 m/s. The diffusive field can be recovered by the correspondence principle with the use of Fourier and inverse Fourier transforms (Mittet, 2010).

PRELIMINARY RESULTS

Differential fictitious waveforms

The differential waveforms for the first 100 recording points of the horizontal magnetic components constructed by subtracting the fictitious waves recorded before performing any hydrofracturing and the records after the first stage is shown as the left panel of Figure 4; while the right panel is for the difference between the records after the 10th stage and the background. It appears that there are more differences in the H_x-component (the traces in black) than in the H_y-component (the traces in red) for the first 100 recording points, which are closer to the origin of the X-Y coordinates.

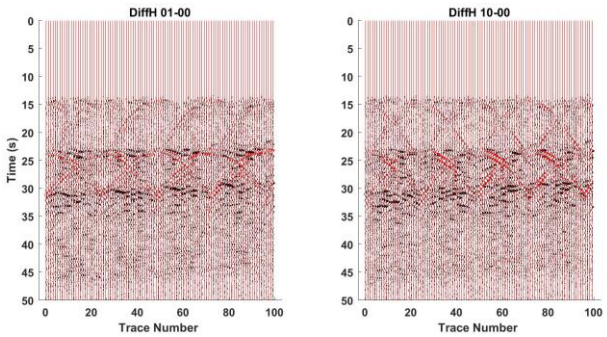

Figure 4. The differences of the magnetic field for the first 100 channels between the background and after hydrofracturing Stage 1 (left panel) and between the background and after hydrofracturing Stage 10 (right panel). The traces in black are for the H_x-component and the traces in red are for the H_y-component.

Difference in apparent resistivity

As we have described above the classical MT sounding consists of simultaneous measurements of the horizontal electric and magnetic components to get the impedance tensor Z_{ij} through:

$$\begin{bmatrix} E_x(\omega) \\ E_y(\omega) \end{bmatrix} = \begin{bmatrix} Z_{xx}(\omega) & Z_{xy}(\omega) \\ Z_{yx}(\omega) & Z_{yy}(\omega) \end{bmatrix} \begin{bmatrix} H_x(\omega) \\ H_y(\omega) \end{bmatrix} \qquad (2)$$

and the apparent resistivity $Z_{ij}^{\ 2}/(\mu\omega)$ (Balasco et al 2004).

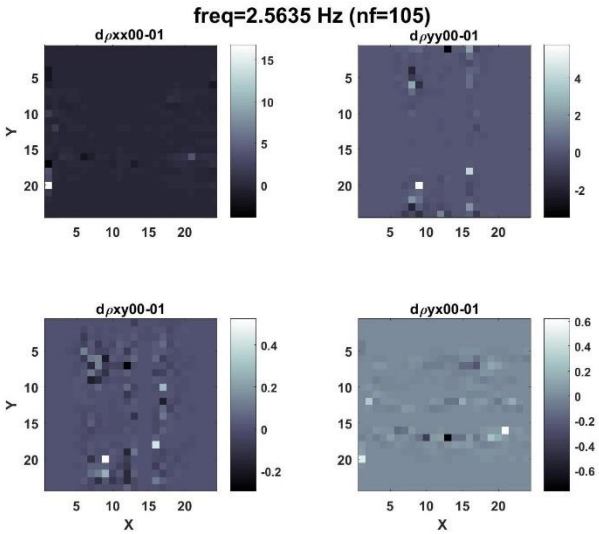

Figure 5. The images of the apparent resistivity differences after Stage 1 and the background at the frequency of 2.56 Hz.

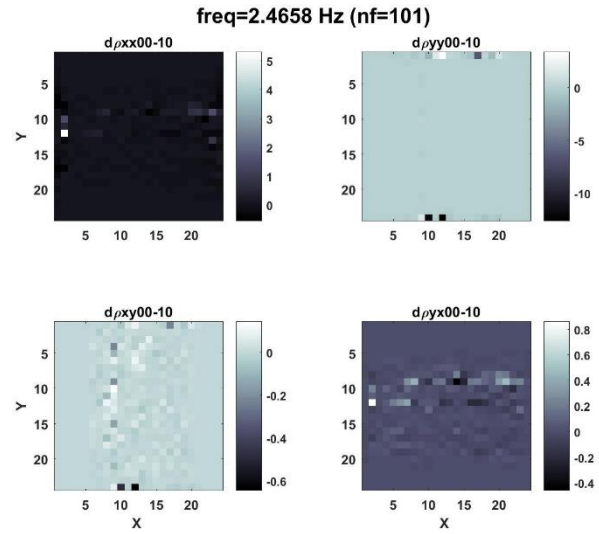

Figure 6. The images of the apparent resistivity differences after Stage 10 and the background at the frequency of 2.47 Hz.

At a given frequency, the difference in the apparent resistivity after the hydrofracturing of Stage 1 and the background is depicted by Figure 5; while the difference in the apparent resistivity after the hydrofracturing of Stages 1-10 and the background is depicted by Figure 6. From Figures 5 and 6 we can see that the cross terms display more pronounced difference than the diagonal terms of the apparent resistivity and deserve more attention.

CONCLUSIONS

Based on the wave-diffusion correspondence principle, we tested the plausibility of using magnetotelluric EM surveys for monitoring the growth of the hydraulically fractured permeable zones by stage advancement by looking into the variations of the electromagnetic parameters by modeling the propagation of the fictitious waves using 3D pseudo-spectral time domain numerical simulation tool and the effective medium theory. The preliminary results reveal that the variation of the EM parameters recorded by a surface array reveal the growth of the highly permeable hydro-fractured zones when the conductivity change caused by the hydrofracturing at xx% level in terms of the effective conductivity.

ACKNOWLEDGMENTS

The first author (LL) thanks the Blaustein Visiting Professorship at Stanford University and Stanford Center for Induced and Triggered Seismicity (SCITS) for their support to this work.

REFERENCES

Abdulaziz A.M., 2013, Microseismic imaging of hydraulically induced-fractures in gas reservoirs: a case study in Barnett shale gas reservoir, Texas, USA, Open Journal of Geology, **3,** 361-369.

Albaric, J., Oye, V., Langet, N., Hasting, M., Lecomte, I., Iranpour, K., Messeiller, M., Reid, P., 2014, Monitoring of induced seismicity during the first geothermal reservoir stimulation at Paralana, Australia, *Geothermics*, **52,** 120-131.

Archie, G., 1942, The electrical resistivity log as an aid in determining some reservoir characteristics, *Trans. A.I.M.E.*, **146,** 54-62.

Balasco, M., V. Lapenna, V., Siniscalchi, A., and Telesca, L., 2004, Stability analysis of apparent resistivity measurement in the seismically active area of Val d'Agri (southern Italy), *Natural Hazards and Earth System Sciences*, **4,** 775–781.

Berryman, J., and Hoversten, G.M. 2010, Modeling electrical conductivity for earth media with macroscopic fluid filled fractures, *Geophysical Prospecting*, **61**, 471–493.

Cuevas, N., 2013, Analytical solutions to dipolar EM sources inside infinite metallic casing. SEG Technical Program Expanded Abstracts 551–555.

Didana, Y., Heinson, G., and Thiel, S., 2016, Magnetotelluric monitoring of hydraulic fracture stimulation at the Habanero Enhanced Geothermal System, Cooper Basin, South Australia, Proceedings of the 23rd Electromagnetic Induction Workshop, Chiang Mai, Thailand.

Glover, P.W.J., 2010, A generalized Archie's law for n phases, *Geophysics*, **75(6),** E247-E265.

He, Z., Hu, Z., Gao, Y., He, L., Meng, C., Yang, L., 2015, Field test of monitoring gas reservoir development using time-lapse continuous electromagnetic profile method, *Geophysics*, **80(2),** WA127-WA134.

Heagy, L., and Oldenburg, D., 2013, Investigating the potential of using conductive or permeable proppant particles for hydraulic fracture characterization. SEG Technical Program Expanded Abstracts 576–580.

Liu, L., and S. Arcone, 2005, Propagation of radar pulses from a horizontal dipole in variable dielectric ground: A numerical approach, *Subsurface Sensing Technologies and Applications*, **6(1),** 5-24.

MacFarlane, J., Thiel, S., Pek, J., Peacock, J., and Heinson, G., 2014, Characterisation of induced fracture networks within an enhanced geothermal system using anisotropic electromagnetic modelling, *Journal of Volcanology and Geothermal Research*, **288,** 1–7.

Maxwell, S.E., Cho, D., Pope T., Jones, M., and Leonard, J., 2011, Enhanced reservoir characterization using hydraulic fracture microseismicity, SPE 140449.

Mittet, R., 2010, High-order finite-difference simulations of marine CSEM surveys using a correspondence principle for wave and diffusion fields, *Geophysics*, **75,** F33-F50.

Nam, M. J., Kim, H. J., Song, Y., Lee, T. J., Son, J. S., and Suh, J. H., 2007, 3D magnetotelluric modelling including surface topography, *Geophysical Prospecting*, **55**, 277–287.

Pandurangan, V., Chen, Z. R., Jeffrey, R.G, Mapping of hydraulic fractures using tiltmeter data for design of EGS stimulation, Proceedings World Geothermal Congress 2015 Melbourne, Australia, 19-25 April 2015

Thiel, S., 2016, Electromagnetic monitoring of hydraulic fracking: relationship to permeability, seismicity and stress, Keynote paper presented at EMIW 2016.

Warpinski, N., 2011, Hydraulic fracture height in gas shale reservoirs. SEG Technical Program Expanded Abstracts 3705–3706.